Journal of Photochemistry and Photobiology 7 (2021) 100056

Contents lists available at ScienceDirect

Journal of Photochemistry and Photobiology

journal homepage: www.sciencedirect.com/journal/journal-of-photochemistry-and-photobiology

Catalase-loaded polymersomes as a promising safe ingredient to active photoprotection

C.A. Oliveira [a,b], C. Forster [b], V. Feitosa [d], A.R. Baby [c], P. Léo [d], C.O. Rangel-Yagui [b,*]

[a] Laboratory of Development and Analytical Validation- Farmanguinhos - Oswaldo Cruz Foundation, Rio de Janeiro, RJ, Brazil
[b] Department of Biochemical and Pharmaceutical Technology - University of São Paulo, Brazil
[c] Department of Pharmacy - University of São Paulo, Brazil
[d] Bionanomanufacturing Center - Institute for Technological Research – IPT, São Paulo, SP, Brazil

ARTICLE INFO

Keywords:
Pluronic L121
Protein drug
Enzyme
Transdermal delivery and sunscreens

ABSTRACT

The topical application of enzymes for UV-induced damage repair, such as catalase, represents an interesting strategy for "active" photoprotection. However, catalase, a large and hydrophilic molecule, needs to penetrate the skin to present activity and, in this sense, nanocarriers can provide an aid for barrier crossing. Among the nanocarriers, polymersomes (Ps) obtained by the self-aggregation of amphiphilic block copolymers represent an alternative for topical enzyme delivery. Here, catalase-loaded Ps of Pluronic® L121, an amphiphilic triblock copolymer, were prepared by direct dissolution and *in vitro* evaluated regarding safety and efficacy. The Ps presented a suitable photo/cytotoxicity profile regarding the sun-damaged epidermis. Pre-clinical safety tests indicated that the HET-CAM assay was more appropriate than cytotoxicity assays to predict the irritant potential of the Ps. Based on cutaneous permeation assays associated with laser scanning confocal fluorescence microscopy, the Ps increased ten times the catalase percentage of skin permeation. Additionally, *in vitro* assays indicated that catalase-loaded Ps were able to eliminate UV-induced lipid peroxidation in deeper layers of the skin (viable epidermis + dermis) in comparison to free catalase. Penetration assays in 3D cell culture and efficacy assays confirmed the preferential delivery of catalase in the deeper layers of the skin owing to the permeation enhancer effect of Pluronic L121 and/or the membrane translocation capacity of the Ps. In conclusion, our findings indicate catalase-loaded Ps as an innovative nanomaterial for active sunscreens.

1. Introduction

An increase in skin cancer incidence has been recorded in recent years, impacting health care systems. One in every three cancer diagnostics refers to skin cancer worldwide and according to the World Health Organization (2020), two to three million non-melanoma skin cancer cases and 132,000 melanoma skin cancer cases occur each year globally. Australia, for example, has high rates that reaches about 80% of all recent cancer cases [1,2]. Topical photoprotection classically involves molecules that absorb or reflect ultraviolet (UV) radiation, such as organic and inorganic UV filters. However, this is considered a passive strategy and does not prevent the effects of constant exposition to UV radiation. Constant exposure to solar radiation triggers inflammatory reactions that promote the increase of free radicals and reactive oxygen species (ROS), what in turn depletes skin enzymes resulting in damage to the DNA, lipid membranes and proteins. Recently, the topical application of antioxidant enzymes has emerged as a strategy for "active photoprotection," filling the current gap in sun protection [3].

Antioxidant enzymes are highly potent and specific for ROS degradation. In addition, enzymes are not consumed in the reaction, whereas nonenzymatic antioxidants are. Catalase, for example, is a tetrameric enzyme of 240 kDa mainly present in the peroxisomes of mammalians that catalyzes the degradation of 40 million molecules of H_2O_2 per second. Several authors described the successful use of catalase to treat inflammatory and dermatological conditions such as vitiligo [4–7]. To be an efficient "active" sunscreen ingredient, catalase must access the living cells of the epidermis, which can be a challenge for a large hydrophilic molecule. The use of drug delivery systems can significantly enhance this enzyme skin penetration. Nonetheless, most of the transdermal delivery systems are not mechanically stable enough to permeate

* Corresponding author at: Carlota de Oliveira Rangel-Yagui, NanoBio – Laboratory of Nanobiotechnology, Department of Biochemical and Pharmaceutical Technology, University of São Paulo, 580 Prof. Lineu Prestes Av., Bl. 16, 05508-900, São Paulo, SP, Brazil.
E-mail address: corangel@usp.br (C.O. Rangel-Yagui).

https://doi.org/10.1016/j.jpap.2021.100056
Received 12 March 2021; Received in revised form 8 June 2021; Accepted 27 July 2021
Available online 29 July 2021

intact across skin without losing their cargo. The stratum corneum (*SC*), the uppermost layer of skin, is responsible for 80% of skin transport resistance. The hydrophobic composition of *SC* serves as an efficient obstacle toward polar compounds, while the living epidermis presents resistance against highly lipophilic compounds. The viable epidermis cells, the corneocytes, are 50-100 nm thick and have a diameter of 30-50nm [13]. Therefore, the size and the ability to squeeze through narrow pores are key parameters in transdermal delivery systems [14]

The use of self-assembly amphiphilic copolymers has been increasing regarding the development of vesicle delivery systems. In this sense, polymersomes (Ps) are polymeric vesicles formed by the self-aggregation of amphiphilic block copolymers. Compared to liposomes, Ps have superior mechanical properties and can resist higher mechanical stresses. In addition to penetration, encapsulation into Ps can also increase the enzyme thermal and physicochemical stability in the final product [14]. More specifically, Ps of Pluronic® L121 ($EO_5PO_{68}EO_5$) are expected to be flexible enough to squeeze across the tight gaps of the skin, owing to the larger size and more loosely packed bilayer [8–12]. Therefore, encapsulation into Ps of Pluronic® L121 (from now on denominated Pluronic L121) could significantly enhance catalase skin penetration.

Recently, our group developed and characterized catalase-loaded Pluronic L121 Ps in a quality by design approach [15]. The vesicles were prepared through direct dissolution and the results provided a design space for the development of suitable topical Ps regarding hydrodynamic diameter ($200 \geq HD \leq 400$), encapsulation efficiency ($2 \geq$ %EE ≤ 5), and polydispersity index ($0.1 \geq PDI \leq 0.3$) as a function of stirring speed (800 rpm), stirring time (h; $40 \geq ST \leq 48$), and catalase concentration (mg/mL; $0.24 \geq CAT \leq 0.40$). In this work, we investigated the pre-clinical profile of the catalase-loaded Pluronic L121 Ps and demonstrated these nanostructures offer a promising alternative for active sunscreen protection.

2. Material and methods

2.1. Materials

Pluronic L121 was kindly donated by BASF Brazil (São Paulo, Brazil). Catalase (lyophilized powder, ≥10,000 units/mg protein), fluorescein isothiocyanate (FITC)-dextran (3-5KDa), batch tested fetal bovine serum (FBS), and Dulbecco's Modified Eagle Medium (DMEM) were purchased from Sigma-Aldrich Brazil (São Paulo, Brazil). SYTO 9 and propidium iodide (PI) were acquired from Thermo Scientific (São Paulo, Brazil). The materials were used without further purification. Ultra purified water (Milli-Q, Millipore, USA) was used in all experiments. Polymersomes were prepared by direct dissolution of 2mg/mL Pluronic in PBS buffer pH 7.4 with stirring speed of 750 rpm, stirring time of 48 h and catalase or FITC-dextran concentration of 0.24 mg/mL [15].

2.2. Safety assays

2.2.1. In vitro cytotoxicity

Cytotoxicity of Ps was evaluated in two cell types by monitoring the neutral red uptake (NRU): mouse fibroblast NCTC 929 (ATCC CCL-1) and rabbit cornea SIRC cells (ATCC CCL-60). After the seeding period, the cells were exposed (24h) to catalase and blank Ps (without catalase), incubated for 3 hours (37 °C, 5% CO_2) with neutral red dye (50 μg/mL), and the extraction was proceeded using ethanol/acetic acid/water (50%/1%/49%). The absorbance of the dye was assessed at 540 nm on a spectrophotometer UV Vis (LabSystemsTitertek Multiskan MCC/340 Plate Reader; Thermo Labsystems, , USA). The negative control was obtained by absorbance of cells exposed only to medium with 5% FBS, and an SDS solution was used as positive cytotoxicity control. The effect of catalase and the Ps on cell viability was estimated in comparison to control cells. The concentration responsible for 50% reduction of cell viability (IC_{50}) was calculated with the help of the Phototox© software version 2.0. The assays were performed in triplicates. [16,17].

2.2.2. In vitro photocytotoxicity

Photocytotoxicity of catalase and Ps in mouse fibroblast NCTC 929 (ATCC CCL-1) (100 μL; 1×10^5cells/mL) was - evaluated by NRU. After the seeding period, catalase and Ps dispersed or diluted in DMEM with 10% FBS were added to the cells. The plates were- incubated for one hour and following half of them were irradiated at 5J/cm^2 for 35 minutes (Suntest® CPS+). The plates were washed and incubated for 24 hours (37 °C, 5% CO_2) in DMEM with 10% FBS (100 μL/mL). Finally, the cells were kept for more 3 hours with neutral red dye (50 μg/mL), and the extraction proceeded with ethanol/acetic acid/water (50%/1%/49%). The absorbance was assessed as described in item 2.2.1. The negative control was obtained by absorbance of cells exposed only to medium and a tetracycline solution was used as the photocytotoxicity positive control. The assays were performed in triplicates and data analyzed with the help of the Phototox© software version 2.0. The photo irritation factor (PIF) was calculated using Eq. 1 and the mean photo effect (MPE) using Eq. 2. [18,19].

$$PIF = \frac{IC_{50}(\ -Irr)}{IC_{50}(\ +Irr)} \tag{1}$$

where IC50 (-Irr) is the concentration of the test substance corresponding to 50% reduction in cell viability without photoirradiation, and IC50 (+ Irr) when irradiated.

$$MPE = \frac{\sum_{i=1}^{n} w_i PEc_i}{\sum_{i=1}^{n} w_i} \tag{2}$$

where the photo effect (PE_{ci}) at the concentration (C) is the product of the response effect (REc) and the dose-effect (DEc), i.e., PEe = REc x DEc, the response effect (REc) is the difference between the responses observed in the absence and presence of light, i.e., REc = Rc (-Irr) - Rc (+Irr).

2.2.3. Irritant potential assay

HET-CAM (hen's egg test-chorioallantoic membrane) test was carried out after nine days of incubation as previously described by Oliveira and collaborators [20,21]. The fertile White Leghorn hen's eggs were provided by Mário Salviato Ovos Férteis (São Paulo, Brazil). The eggshell was cut at the marked air sac, and the membrane was exposed. The outer membrane was carefully removed using tweezers, so the CAM (chorioallantoic membrane) was exposed. The positive control for vascular hemorrhage and lysis was a 1.0% SDS solution (300 μL), and 0.9% NaCl solution (300 μL) was the negative control. Samples of 300 μL of catalase-loaded Ps and blank Ps were also applied [5]. For the analyses, the samples were recorded for 300 seconds regarding any event (hemorrhage, lysis, and coagulation). Assays were carried out in triplicate and the irritation score values were evaluated based in Eq. 3, with samples graded regarding irritancy score: 0-0.9 = non-irritant; 1-4.9 = slightly irritant; 5-8.9 = moderately irritant; 9-21 = strongly irritant.

$$300[IS] = 5[301 - H] + 7[301 - L] + 9[301 - C] \tag{3}$$

where IS: irritation score; H: onset time in seconds for the start of hemorrhage; L: onset time in seconds for the start of lysis; C: onset time in seconds for the start of coagulation.

2.3. Skin permeation analysis by laser scanning confocal fluorescence microscopy

Skin permeation was determined in pig ears. The underlying cartilage was removed from the skin and stored in a freezer. Experiments (n = 3) were performed on glass Franz-type diffusion cells with a diffusional area of 1.54 cm^2. The receptor compartment had PBS (pH 7.4), at 32.0 °C ± 1.0 °C and 130 rpm. One milliliter of the samples - purified

FITC-dextran loaded Ps (16 μg/mL), unpurified FITC-dextran loaded Ps (0.24 mg/mL) and FITC-dextran solution (~ 0.4 mg/mL) - were used in the donor compartment. At the donor container, occlusive devices were prevented [21]. After 24h, each area in contact with the product was washed thoroughly with phosphate buffer (3 times). The samples were frozen appropriately (Thermo Scientific Richard-Allan Scientific Neg-50) and then cut in sections of 10-40 μm in a cryomicrotome (HM525 NX Cryostat, Thermo Scientific®) for further analysis by laser scanning confocal fluorescence microscopy (LSM 700, Zeiss) , with excitation at 488 nm and emission at 555 nm. The fluorescence intensity was estimated with the help of the Image J software and the % fluorescence intensity/area of each sample was calculated for the *stratum corneum* and viable epidermis + dermis. The analyses were performed in triplicate.

2.4. Tissue penetration in 3D cell culture models by laser scanning confocal fluorescence microscopy

For this study, mouse fibroblast NCTC 929 (ATCC CCL-1) (1×10^7cells/mL) was used to prepare the three-dimensional (3D) cell culture spheroids by the hanging spherical drop method (25 μL/drop). Cells were nurtured for 24 hours at 37 °C, 5% CO_2 and once formed, the spheroids were moved to a 96-well plate, followed by the addition of 100 μL of DMEM [22]. Purified Ps samples containing FITC-dextran (5% encapsulation efficiency, 16 μg/mL) and FITC-dextran solution in equivalent concentrations (16 μg/mL in phosphate buffer) were added (100 μL) to the wells containing the spheroids and incubated for 24 hours (37 °C, 5% CO_2). Phosphate buffer was used as a negative control. After this period, the medium was removed; and 100 μL of medium containing PI (200 μM) and SYTO 9 (33.4 μM) probes was added to well corresponding to the negative control spheroids. The same volume of medium containing PI (200μM) was added to the other wells, the plate incubated for one hour. Finally, the samples were fixed with a paraformaldehyde solution (4% w/v) for further analysis by laser scanning confocal fluorescence microscopy (LSM 510 Meta, Zeiss)). The studies were performed in triplicates.

2.5. In vitro antioxidant activity of the skin

In this experiment, we investigated Ps samples containing catalase (0.24 mg/mL) and catalase solution in equivalent concentration (0.24 mg/mL in phosphate buffer), and proceeded as described in item 2.3 regarding the skin penetration parameters and sample application. After 24 hours, we progressed to the irradiation of the skin samples (n = 3) performed at the Atlas Suntest® CPS + simulator with a xenon lamp (1500 W) with a dose of 5506 KJ/m2 (765 W/m2). The stratum corneum was then separated by tape stripping (20 times), and the skin was cut into small sections with scissors. The tape and skin were placed in 10 mL methanol. Further, the samples were immersed in an ultrasound bath for 15 minutes and filtered with a 0.45 μm membrane [21]. The analytical steps were detailed by Santos and et al. (2021) in a previous work by our group. Detection of the complex thiobarbituric acid (TBA) with malondialdehyde(MDA) was performed at 532nm using a diode-array UV detector (Shimadzu, Japan) [23]. The retention time (RT) was 5.9 min. The standard curve (peak area = 825858 x [MDA-$(TBA)_2$] + 44687 , R^2 = 0.9956] was established from the MDA solution from the acid hydrolysis of 1,1,3,3-tetramethoxypropane (TEP) [24,25].

2.2.7. Statistical analysis

Minitab (version 16) software performed the statistical analyses with a significance level of 5.0% (α = 0.05). Data were treated using one-way ANOVA followed by the Tukey test for multiple comparisons, the 2-sample t-test, and paired t-test.

3. Results and discussion

Pluronic L121 Ps with and without catalase were obtained by direct dissolution and purified by size exclusion chromatography (SEC), as previously described by our group [15]. For the fluorescence microscopy , FITC-dextran was encapsulated at the same concentrations and conditions as catalase and the Ps obtained preserved similar properties regarding size (~ 300 nm), polydispersity index (~ 0.180) and encapsulation efficiency (~ 5%). Here, we analyzed the efficacy and safety of these nano ingredients by *in vitro* methods.

Safety evaluation of nano-ingredients in cosmetic products is a current matter of debate among regulatory agencies and the scientific community. The toxicological profile of nanoparticles lacks studies and specific tests have not yet been developed. Therefore, the available studies consist in adjustments of already known *in vitro* and *in vivo* tests to understand the mechanisms of the toxicological action of nanomaterials [26]. We performed pre-clinical safety studies for blank Ps and catalase solution. After 24h hours of incubation, catalase did not present any *in vitro* cytotoxic effect on SIRC and NCTC 929 cells, as shown in Fig. 1. However, blank Ps decreased SIRC and NCTC 929 cell viability in a concentration-dependent manner. Pluronic L121 presented better cytotoxicity profile than SDS in NCTC 929 (a regulatory recommended cell lineage). The IC_{50} values were 83.3 ± 8.3 μg/mL and 26.0 ± 4.2 μg/mL, respectively. In other words, the copolymer is significantly less toxic to the cells that the positive control SDS, a classic anionic surfactant. On the other hand, the IC_{50} on SIRC cells was 49.6 ± 13.5 μg/mL for Pluronic L121 and 56.6 ± 1.5 μg/mL for the positive control (SDS). Apparently, the value observed for Pluronic L121 is close to the value of the positive control SDS. However, Yang and co-workers tested the cytotoxicity profile of Pluronic L121 in human foreskin fibroblast at high concentrations (from 0.025 to 0.2% wt/wt) and could not determine the copolymer IC_{50} value [27]. This difference in IC_{50} can be explained by the differences in cell lineages and also by the dye used in the cytotoxicity assay (MTT or NRU). According to the literature, NRU assay better estimates anionic detergents, and MTT is suitable for analyzing a range of distinct structural surfactants [28]. Here, we decided to use NRU to meet the regulatory standards for the phototoxicity assay (OECD 432 In vitro 3T3 NRU phototoxicity test), and kept the same procedures for the cytotoxicity assay (ISO 10993-5, Biological evaluation of medical devices-part 5: tests for cytotoxicity:*in vitr* methods). Therefore, our results can be better compared to others previously published or future ones. Nonetheless, they point for the need to consider complimentary methods to estimate cytotoxicity.

Bracher and co-workers described standard irritation scores based on the IC_{50} of chemical substances in general. According to the IC_{50} value, materials are classified as strongly irritant (< 7 μg/mL); slightly irritant (≥ 7 ≤ 175 μg/mL) and non-irritant (> 175 μg/mL). Based on this classification, Pluronic L121 and SDS are considered slightly irritant for both cell lineages [29]. Nonetheless, it is well known that SDS, as an anionic surfactant, is a skin irritant and, in general, amphiphilic copolymers as Pluronic L121 are less irritant than ionic surfactants [30]. This result reinforces the need to study the toxicity profile of pharmaceutical ingredients by more than one method.

Regarding the photocytotoxicity profile of the samples (Fig. 2, Table 1), the results indicated the blank Ps as not phototoxic. Based on the validation study by Spielmann (1998), substances presenting PIF < 2 or MPE < 0.1 are classified as non-phototoxic; 2 < PIF < 5 or 0.1 < MPE < 0.15 as probably phototoxic; and PIF > 5 or MPE > 0.15 as phototoxic [18,31] (OECD, 2004; SPIELMANN et al., 1998). As an endogenous enzyme with an essential role in photodamage repair and no target structural alert for phototoxicity, catalase did not reduce cell viability with or without radiation, as expected.

To reinforce our results on the cytotoxicity of the Ps and catalase, the HET-CAM test was also performed. The HET-CAM assay allows evaluating vascular effects since the acute effects induced by a substance on small blood vessels and proteins of this soft tissue membrane can be used

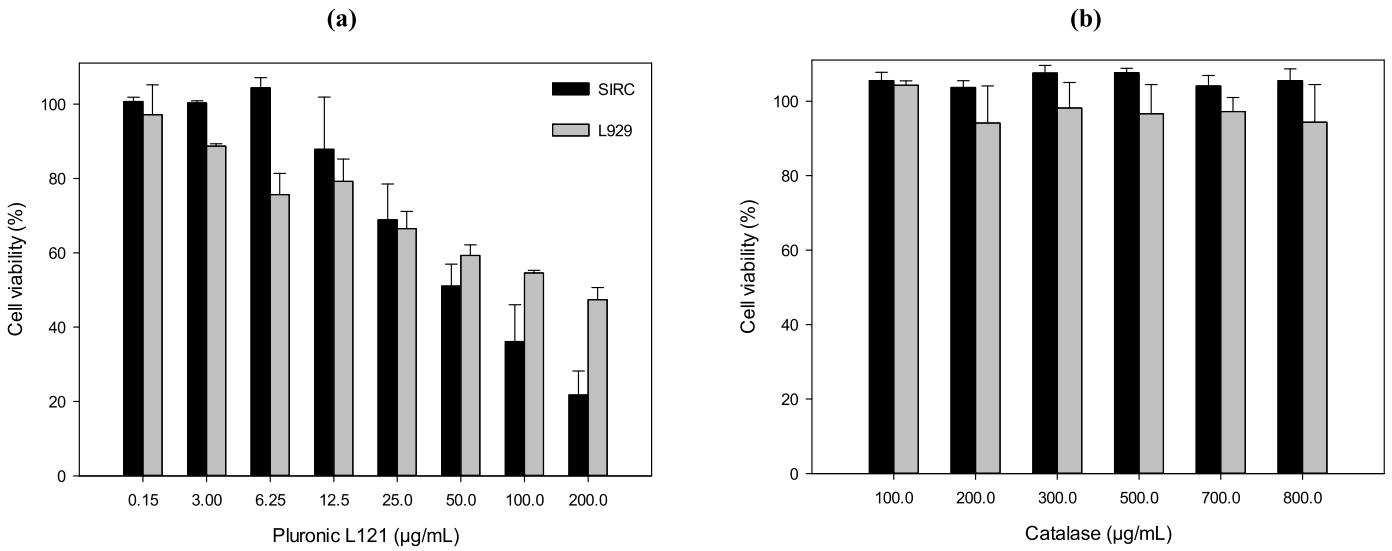

Fig. 1. Viability of L929 (mouse fibroblasts) and SIRC (rabbit cornea cells) after exposure to **(a)** blank Pluronic L121 polymersomes and **(b)** catalase solution. Cell viability was estimated by uptake of neutral red assay using not treated cell as control (100%). The error bar corresponds to standard deviations of three experiments.

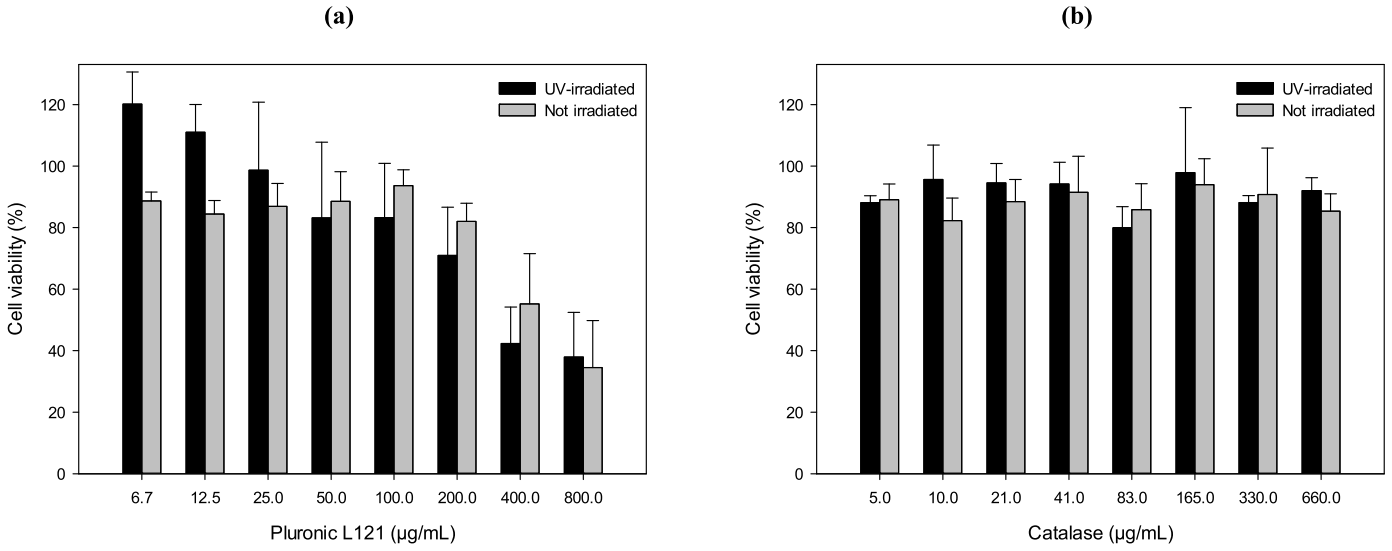

Fig. 2. Viability of L929 (mouse fibroblasts) cells after exposure to **(a)** blank Pluronic L121 polymersomes and **(b)** catalase solution, followed by UV-irradiation or not. Cell viability was estimated by uptake of neutral red assay using not treated cell as control (100%). The error bar corresponds to standard deviations of three experiments.

Table 1
Photo Irritation Factor and Mean photo effect (mean values ± standard desviation).

	Photo Irritation Factor	Mean photo effect
Catalase	1 ± 0	0.04 ± 0.008
Blank polymersome	1.56 ± 0.3	- 0.152 ± 0.1
tetracycline	0.16 ± 0.06	46.6 ± 4.4

to indicate the irritancy profile generated by the tested substance. The ingredient is applied directly to the CAM of fertilized hen eggs and acute effects such as hemorrhage, lysis of blood vessels and coagulation are assessed. The chorioallantoic membrane (CAM) is highly vascularized and, therefore, HET-CAM can be an interesting assay to determine the irritant ability of ingredients as Ps [21,32]. For instance, the correlation of *in vivo* irritancy data and HET-CAM for gelatin nanoparticles was already described [21]. Also, an adequate safety prediction by HET-CAM in comparison to *in vitro* cytotoxicity profile in human keratinocytes was described [33]. Here, the SDS solution was identified as a strong irritant (11.77 ± 0.05 irritants score) as hemorrhage and lysis were observed (Fig. 3). Based on the irritancy score, blank Ps (0 irritancy score) and catalase-loaded Ps (0 irritancy score) were graded as non-irritant due to the no detection of vascular effects.

The combined analysis of the *in vitro* cytotoxicity of Pluronic L121 Ps indicates these novel catalase-loaded polymeric vesicles are safe for topical application and could be seen as a promising ingredient for active photoprotection.

The permeation assays were performed to understand how the Ps would interact or deliver ingredients through the skin. For a molecule to permeate across the skin, it must have a suitable permeation profile correlated with several parameters such as logP, molecular weight, ionization state, hydrogen bond capacity, and solubility. Regarding transdermal formulations, especially, the ability to deform through the epithelial gaps is desirable. We studied the cutaneous penetration/permeation of Pluronic L121 Ps containing the FITC-dextran fluorescent

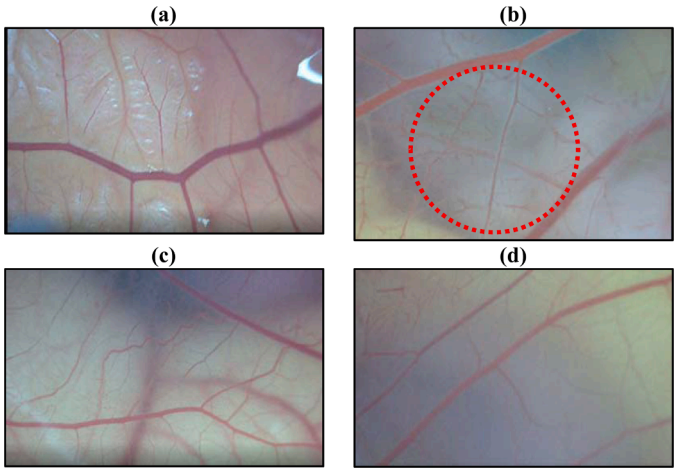

Fig. 3. Sequence of photographs showing **(a)** the egg chorioallantoic membrane (CAM) before assay and after five minutes of exposure to each sample: **(b)** SDS solution, **(c)** blank Pluronic L121 polymersomes and **(d)** catalase-loaded polymersomes. The red highlighted circle indicates the lysis of vessels.

probe. Figs. 4 and 5 indicate that FITC-dextran, as expected, tends to deposit almost exclusively in the stratum corneum since molecules with MW above 500 Da usually do not penetrate the skin. The lipid composition of the stratum corneum distinguishes it from the other biological barriers as a good obstacle for hydrophilic compounds. On the contrary, hydrophobic ingredients find a more resistant environment at the viable layers of the epidermis [34].

The FITC-dextran loaded Ps without purification resulted in an increase from less than 1% to 15% of total fluorescence in the viable epidermis + dermis layers (Fig. 5). However, we must consider that only 5% of the probe was incorporated into the nanostructures, and 95% of the probe remained free in solution. In this sense, topical formulations containing nonionic copolymers, such as Pluronic L121, may alter the skin penetration profile of some compounds. This copolymer is capable of penetrating intercellular gaps of the *SC* and eventually solubilizing and removing elements of this structure. Also, its presence in the intracellular matrix and interaction with keratin filaments can result in corneocytes rupture. The stratum corneum is organized as a combination of keratinized cells embedded in a lipid matrix as a "bricks and mortar" arrangement. The "bricks" correspond to the keratinocytes and "mortar" to the content of the lamellar granules, containing lipids and proteins. Pluronic L121 can also emulsify the lipophilic content allowing hydrophilic molecules to penetrate deeper layers of the viable epithelium. Additionally, Pegoraro *et al.* (2014) proposed that Ps composed of $PMPC_{25}$- $PDPA_{70}$, $PMPC_{25}$-$PDPA_{500}$,poly(2-(methacryloyloxy)ethylphoshorylcholine)-co-poly(2(diisopropylamino)ethylmethacrylate) and PEO_{113}-$PDPA_{70}$, poly(ethyleneoxide)-co-poly(2-(diisopropylamino) ethyl methacrylate) are large and flexible structures that could deform and translocate through narrow pores, without morphological changes. Larger Ps (~ 400nm) would be more flexible than smaller ones (100 - 200 nm), considering the large surface area compared to the membrane thickness and its effect on surface tension [35]. Regarding the triblock copolymer Pluronic L-121, the different architecture with no defined bilayer assembly shape (both I- and U-shaped are suitable) results in large vesicles with a loosely packed bilayer that could also be flexible and translocate across pores [12,36]. For the purified sample, in which no free probe should be present, the % fluorescence intensity/area detected in the *SC* and living epidermis was equivalent, reinforcing the possibility of translocation.

Our focus in this work is to deliver enzymes to the skin, nonetheless the results in the 2D cell culture model pointed out for a possible penetration effect of the polymersomes and this could also be interesting for other applications, such as the delivery of therapeutic proteins/enzymes to solid tumors. Therefore, we decided to investigate the Ps in a 3D cell culture model. The *in vitro* 3D cultures solve the weaknesses of 2D systems, allowing cell-cell/extracellular and matrix-cell interactions, which are fundamental to regulate cellular behavior and function [37].

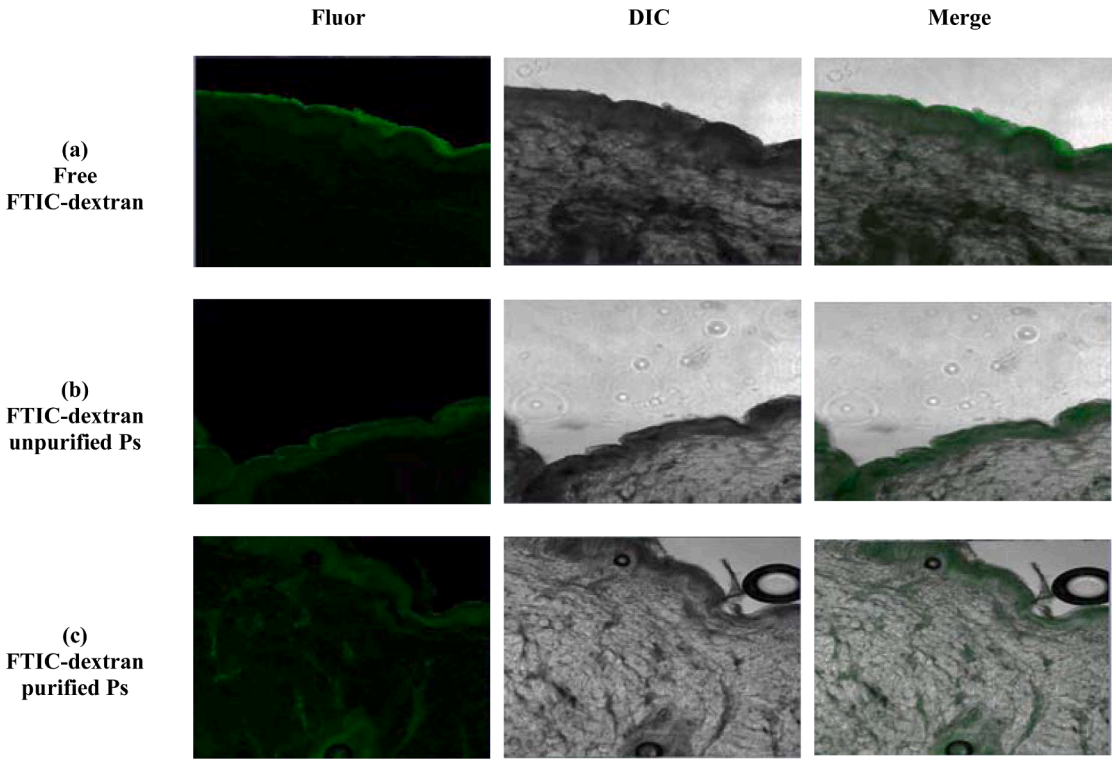

Fig. 4. Laser scanning confocal fluorescence microscopy of pig skin after 24 hours permeation with **(a)** free FTIC-dextran solution, **(b)** unpurified FTIC-dextran loaded Pluronic L121 polymersomes (Ps) and **(c)** purified FTIC-dextran loaded Pluronic L121-Ps. Fluor: fluorescence, DIC: differential interference contrast.

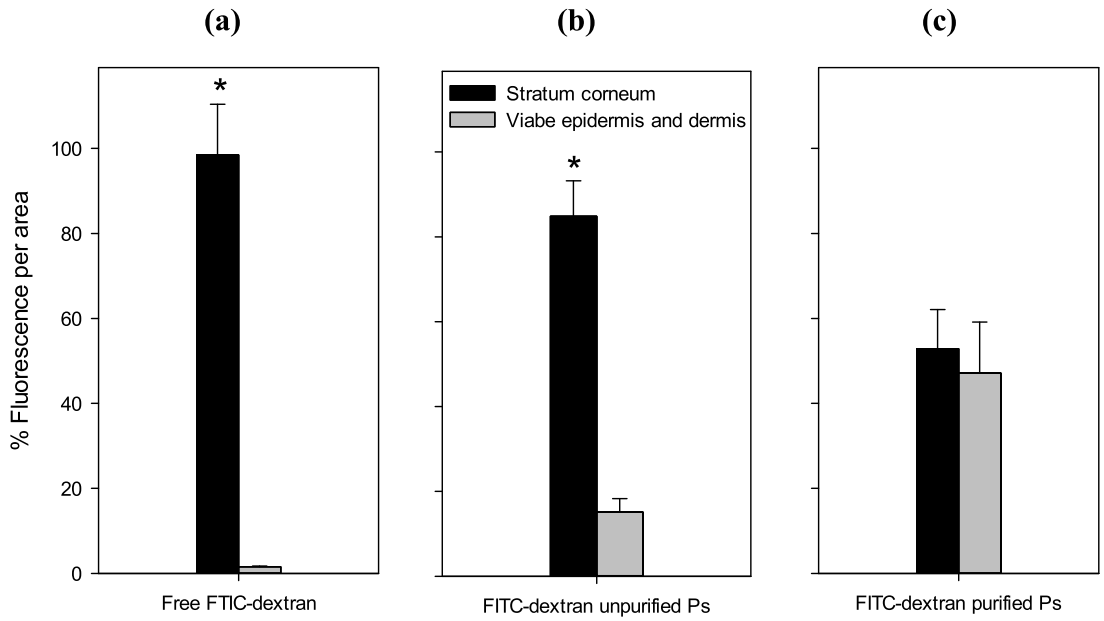

Fig. 5. Fluorescence intensity per area of pig skin layers (stratum corneum, viabe epidermis and dermis) after 24 hours permeation with **(a)** free FTIC-dextran solution, **(b)** unpurified FTIC-dextran loaded Pluronic L121 polymersomes (Ps) and **(c)** purified FTIC-dextran loaded Pluronic L121-Ps. *Indicates statistically significant differences between skin layers ($p<0,05$). The error bar corresponds to standard deviations of three measuments using the Image J software.

Fig. 6 indicates the viability of the spheroids without treatment (negative control sample) by the intense visualization of the SYTO 9 fluorescent probe [38]. For the spheroids incubated with FITC-dextran loaded Ps, a superficial cell death area strongly marked by the PI fluorescent probe is visualized after 24h. PI is a red fluorescence probe that works by intercalating cellular DNA in dead cells [38]. The 2D cell culture assay earlier presented in this work already indicated a dose-dependent cytotoxic effect of Pluronic L121.

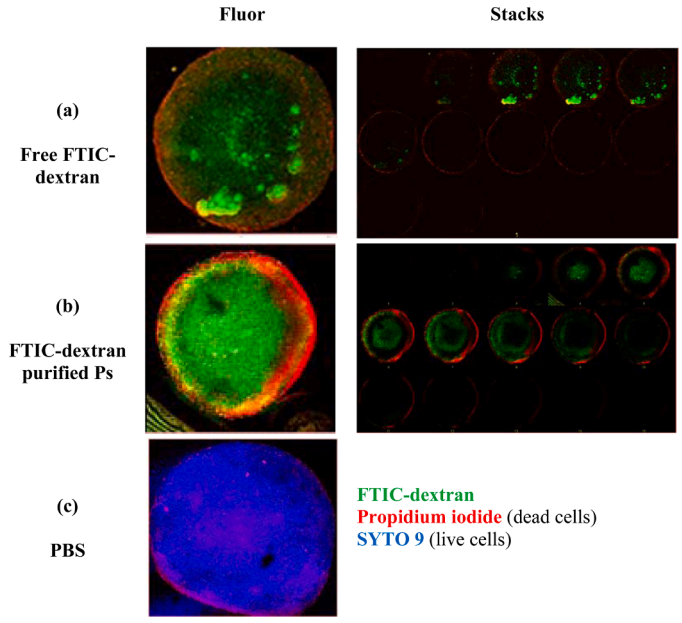

Fig. 6. Laser scanning confocal fluorescence microscopy of L929 fibroblastic spheroids incubated for 24 hours with **(a)** free FTIC-dextran solution, **(b)** purified FTIC-dextran loaded Pluronic L121 polymersomes (Ps) and **(c)** PBS as negative control. The samples **(a)** and **(b)** were stained with propidium iodide to access dead cells, whereas sample **(c)** was stained with propidium iodide and SYTO 9 probe indicating dead and live cells respectively.

FITC-dextran is generally used in cell permeability assays and its mechanism of cellular internalization is widely described [39]. Schnatwinkel *et al.* (2004) described the non-specific mechanism of fluid-phase endocytosis for the internalization of FITC-dextran in fibroblasts (NIH3T3). These conclusions are in agreement with our results (Fig. 6) since we observed the presence of fluorescence inside spheroids incubated with the FITC-Dextran solution [40]. These results are confirmed by the assembly of the stacks of PI and FITC-Dextran channels, where it is not possible to observe regions marked in an overlap.

The translocation profile through membranes, assigned to Ps, was used by Colley *et al.* (2014) to confirm the capacity of Ps to penetrate multicellular tumor spheroids [41]. This profile is also observed in Fig. 6, in which higher fluorescence of FITC-dextran inside the spheroid incubated with the loaded Ps is observed without compromising the cellular viability of the inner layers of the cell cluster.

Finally, we investigated the *in vitro* antioxidant potential of the epidermis after the topical application of a catalase solution and catalase-loaded Ps in both the SC and the viable epidermis + dermis by quantification of the addition product formed in the reaction of MDA and TBA. The incidence of UV radiation on the skin increases oxidative damage through the formation of species as superoxide anion, hydrogen peroxide, hydroxyl radical and singlet oxygen. The degree of lipid peroxidation, correlated to the photodamage, can be measured by the presence of its degradation products, such as MDA [42].

According to Fig. 7, similar values of lipid peroxidation for pig skin samples in PBS were obtained for the upper skin layer (*SC*) with or without exposition to UV irradiation. Also, the *SC* already has an initial peroxidation profile before sample irradiation and did not increase with the irradiation dose proposed for this work in the negative control (saline). The lipid peroxidation profile of the *stratum corneum* can be explained by the high content of lipids in its composition as opposed to the viable epidermis + dermis, a region where endogenous antioxidant enzymes such as catalase are located. Muramatsu *et al* (2005) demonstrated that the expression of catalase in the cytoplasm of keratinocytes (granular layer) in rats was coordinated by the generation of UV-induced hydrogen peroxide [43]. In deeper layers (viable epidermis + dermis), on the other hand, lipid peroxidation products were only present after irradiation. For the samples treated with free catalase, no lipid peroxidation product was detected in either *SC* or the viable epidermis

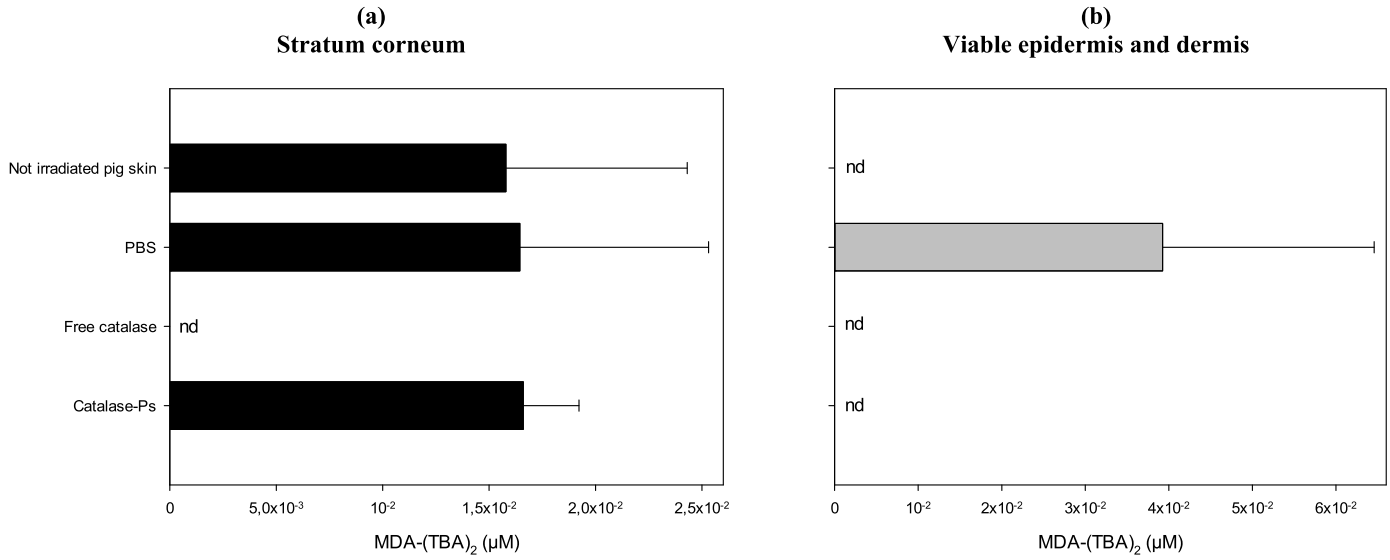

Fig. 7. Quantification of the MDA-$(TBA)_2$ adduct into **(a)** stratum corneum and **(b)** viable epidermis and dermis of pig skin after 24 hours treatment with catalase solution, catalase-loaded Pluronic L121 polymersomes (Ps) and PBS, followed by UV-irradiation. Not irradiated pig skins were used as control. The error bar corresponds to standard deviations of three analysis. MDA: malondialdehyde; TBA: thiobarbituric acid; nd: peak not detected.

+ dermis, while catalase-loaded Ps treatment showed the absence of lipid peroxidation product only in viable epidermis + dermis. Therefore, the catalase solution was able to eliminate the generation of lipid peroxidation products throughout the epidermis. Although this assay does not determine the cutaneous penetration/permeation profile of catalase, it is possible to suggest the low hydrodynamic diameter of the enzyme (~10nm) is responsible for its diffusion and depletion of hydrogen peroxide. The *SC* symbolizes the first significant barrier against skin penetration of pathogens and chemicals. But molecules of less than 40 nm can, to some extent, pass through this layer [44].

Surprisingly, samples treated with catalase-loaded Ps showed lipid peroxidation products in the stratum corneum but the MDA-(TBA)2 adduct was not detected in the deeper layers of the skin. As we discussed earlier, for FITC-dextran-loaded Ps we visualize the probe in the *SC*, in spite of the higher florescence in the deepest layers. We speculate FITC-dextran, as a significantly smaller molecule than catalase, could be leaking from the polymersomes at the *SC*, while catalase not. We should also consider Pluronic L121 might have slightly different penetration effect in both molecules, since catalase is a protein and FITC dextran a carbohydrate-based polymer. Nonetheless, we can assume a preferential delivery to the deepest layers of the skin. Two main reasons could explain this preferential delivery of Ps: (i) the permeation enhancer profile of Pluronic L121 and (ii) the membrane translocation capacity attributed to the Ps [35,45]. While the ability of nonionic surfactants and polymers to enhance some molecules permeation is already well described, further experiments should be used to prove if translocation is taking place, such as the use of labeled vesicles and image detection. Nonetheless, both effects could justify the use of Pluronic L121 Ps for the indirect treatment of UV damage on the skin by reactive oxygen species inactivation. As a perspective, owing to the unique profile of preferential delivery in deeper layers of the epidermis, these nanostructures could also be very useful to encapsulate agents capable of direct repair of UV damage in DNA.

4. Conclusion

In this paper, we showed that polymersomes of Pluronic L121 present low photo/cytotoxicity and can be considered a safe alternative to develop topical formulations for application on UV-exposed skin, as well as for protein delivery. In addition, we showed that catalase-loaded Pluronic L121 Ps enhance antioxidant skin protection especially in the deepest layers of the skin. In other words, these nanostructures increase the catalase action in the viable epidermis + dermis, either by a permeation enhancing effect and/or a translocation mechanism. These findings make catalase-loaded Ps a promising alternative for the future of delivery systems for active photoprotection.

Declaration of Competing Interest

None.

Acknowledgments

The authors acknowledge the National Council for Scientific and Technological Development (CNPq, Process # 301832/2017-0),the São Paulo Research Foundation (FAPESP, processes 2016/03887-4) and the IPT Foundation.

References

[1] D.S. Rigel, Cutaneous ultraviolet exposure and its relationship to the development of skin cancer, J. Am. Acad. Dermatol. (2008) 58.
[2] WHO Ultraviolet radiation available online: http://www.who.int/uv/en/. 2021.
[3] M. Megna, S. Lembo, N. Balato, G. Monfrecola, Active" photoprotection: sunscreens with DNA repair enzymes. A review of the literature, G. Ital. Dermatol. Venereol. 152 (2017) 1–6.
[4] K. Kostovic, Z. Pastar, A. Pasic, R. Ceovic, Treatment of vitiligo with narrow-band UVB and topical gel containing catalase and superoxide dismutase, Acta Dermatovenerol. Croat. 15 (2007) 10–14.
[5] K.U. Schallreuter, H. Rokos, Vitix–a new treatment for vitiligo? Int. J. Dermatol. 44 (11) (2005) 969–970, 2005, 4632, 969–970.
[6] C. Qi, Y. Chen, Q.Z. Jing, X.G. Wang, Preparation and characterization of catalase-loaded solid lipid nanoparticles protecting enzyme against proteolysis, Int. J. Mol. Sci. 12 (2011) 4282–4293.
[7] E. Hood, E. Simone, P. Wattamwar, T. Dziubla, V. Muzykantov, Nanocarriers for vascular delivery of antioxidants, Nanomedicine 6 (2011) 1257–1272.
[8] S. Hocine, D. Cui, M.-N. Rager, A. Di Cicco, J.-M. Liu, J. Wdzieczak-Bakala, A. Brûlet, M.-H. Li, Polymersomes with PEG corona: structural changes and controlled release induced by temperature variation, Langmuir 29 (2013) 1356–1369.
[9] J.S. Lee, J. Feijen, Polymersomes for drug delivery: design, formation and characterization, J. Control. Release 161 (2012) 473–483.
[10] J.D.A. Pachioni-Vasconcelos, A.M. Lopes, A.C. Apolinário, J.K. Valenzuela-Oses, J. S.R. Costa, L.D.O. Nascimento, A. Pessoa, L.R.S. Barbosa, C.D.O. Rangel-Yagui, Nanostructures for protein drug delivery, Biomater. Sci (2016).
[11] A. Pitto-Barry, N.P.E. Barry, Pluronic block-copolymers in medicine: from chemical and biological versatility to rationalisation and clinical advances, Polym. Chem. 5 (2014) 3291–3297.

[12] R. Rodríguez-García, M. Mell, I. López-Montero, J. Netzel, T. Hellweg, F. Monroy, Polymersomes: smart vesicles of tunable rigidity and permeability, Soft Matter 7 (2011) 1532.
[13] C.A. de Oliveira, M.F. Dario, Bioactive cosmetics, Handb. Ecomater. 5 (2019) 3537–3559.
[14] C. Pegoraro, S. MacNeil, G. Battaglia, Polymersome macromolecule delivery across intact human skin, Tech. Proc. 2011 NSTI Nanotechnol. Conf. Expo, NSTI-Nanotech 2011 3 (2011) 428–431.
[15] C.A. Oliveira, C. Forster, P. Léo, C. Rangel-Yagui, Development of triblock polymersomes for catalase delivery based on quality by design environment, J. Dispers. Sci. Technol. 0 (2020) 1–10.
[16] International Organization for Standardization, ISO 10993-5, Biologi- cal evaluation of medical devices-part 5: tests for cytotoxicity: in vitro methods, ISO, Geneva, 1992.
[17] R. Salomoni, P. Léo, A.F. Montemor, B.G. Rinaldi, M.F.A. Rodrigues, Antibacterial effect of silver nanoparticles in Pseudomonas aeruginosa, Nanotechnol. Sci. Appl. 10 (2017) 115–121.
[18] OECD OECD, 432 – In Vitro 3T3 NRU phototoxicity test, in: Organization for Economic Cooperation and Development. Guideline for testing of chemicals. Adopted 13th April 2004.- Organization for Economic Cooperation and Development. Guideline for testing of chemica, 2004, pp. 1–15. ISBN 9789264071162.
[19] S. Alarifi, D. Ali, A. Verma, S. Alakhtani, B. Ali, a Cytotoxicity and genotoxicity of copper oxide nanoparticles in human skin keratinocytes cells, Int. J. Toxicol. 32 (2013) 296–307.
[20] M.F. Dario, C.A. Oliveira, L.R.G. Cordeiro, C. Rosado, I.D.F.A. Mariz, E. Maçôas, M. S.C.S. Santos, M.E. Minas da Piedade, A.R. Baby, M.V.R. Velasco, Stability and safety of quercetin-loaded cationic nanoemulsion: In vitro and in vivo assessments, Colloids Surf. A Physicochem. Eng. Asp. (2016) 506.
[21] C.A. de Oliveira, M.F. Dario, F.D. Sarruf, I.F.A. Mariz, M.V.R. Velasco, C. Rosado, A.R. Baby, Safety and efficacy evaluation of gelatin-based nanoparticles associated with UV filters, Colloids Surf. B Biointerfaces 140 (2016) 531–537.
[22] G. Settanni, J. Zhou, T. Suo, S. Schöttler, K. Landfester, F. Schmid, V. Mailänder, A novel hanging spherical drop system for the generation of cellular spheroids and high throughput combinatorial drug screening, Biomater. Sci. Manuscr. 1 (2016) 1–3.
[23] Y.L. Hong, S.L. Yeh, C.Y. Chang, M.L. Hu, Total plasma malondialdehyde levels in 16 Taiwanese college students determined by various thiobarbituric acid tests and an improved high-performance liquid chromatography-based method, Clin. Biochem. 33 (2000) 619–625.
[24] A.S. Bastos, A.P.D.M. Loureiro, T.F. Oliveira, S.C.T. De; Corbi, R.M.S. Caminaga, C. Rossa, S.R.P. Orrico, Quantitation of malondialdehyde in gingival crevicular fluid by a high-performance liquid chromatography-based method, Anal. Biochem. 423 (2012) 141–146.
[25] J.H.P.M. Santos, C.A. Oliveira, B.M. Rocha, G. Carretero, C.O. Rangel-Yagui, Pegylated catalase as a potential alternative to treat vitiligo and UV induced skin damage, Bioorganic Med. Chem. 30 (2021), 115933.
[26] UNITED STATES Food and Drug Administration, Department of Health and Human Services, Guidance for Industry Safety of Nanomaterials in Cosmetic, 2014, pp. 1–16.
[27] T.F. Yang, C.N. Chen, M.C. Chen, C.H. Lai, H.F. Liang, H.W. Sung, Shell-crosslinked Pluronic L121 micelles as a drug delivery vehicle, Biomaterials 28 (2007) 725–734.
[28] Kortmg, H.C.; Schindler, S.; Hartinger, A.; Kerscher, M.; Angerpointner, T.; Maibach, H.I.; Klinik, D.; Hck, L. MTT-assay and neutral red release (NRR)-assay: relative role in the prediction of the irritancy potential of surfactants. 1994, 55, 533–540.
[29] M Bracher, C Faller, J.R.C. Spengler, Comparison of in vitro cell toxicity with in vivo eye irritation, Mol. Toxicol. 1 (1987) 561–570.
[30] P. Tachon, J. Cotovio, K.G. Dossou, M. Prunieras, Assessment of surfactant cytotoxicity: comparison with the Draize eye test, Int. J. Cosmet. Sci. 11 (1989) 233–243.
[31] H. Spielmann, M. Balls, J. Dupuis, W.J. Pape, G. Pechovitch, O.De Silva, H Holzhu, The international EU /COLIPA in vitro phototoxicity validation study : results of phase II (Blind Trial), Part 1 : The 3T3 NRU Phototoxicity Test 12 (1998) 305–327.
[32] S. Kalweit, R. Besoke, I. Gerner, H. Spielmann, A national validation project of alternative methods to the Draize rabbit eye test, Toxicol. In Vitro 4 (1990) 702–706.
[33] C.A. de Oliveira, D.A. Peres, F. Graziola, N.A.B. Chacra, G.L.B. de Araújo, A. C. Flórido, J. Mota, C. Rosado, M.V.R. Velasco, L.M. Rodrigues, et al., Cutaneous biocompatible rutin-loaded gelatin-based nanoparticles increase the SPF of the association of UVA and UVB filters, Eur. J. Pharm. Sci. 81 (2016) 1–9.
[34] A.C. Watkinson, A.L. Bunge, J. Hadgraft, M.E. Lane, Nanoparticles do not penetrate human skin - a theoretical perspective, Pharm. Res. 30 (2013) 1943–1946.
[35] C. Pegoraro, D. Cecchin, J. Madsen, N. Warren, S.P. Armes, S. MacNeil, A. Lewis, G. Battaglia, Translocation of flexible polymersomes across pores at the nanoscale, Biomater. Sci. 2 (2014) 680–692.
[36] A.C. Apolinário, R.B. Ferraro, C.A. de Oliveira, A. Pessoa, C. de Oliveira Rangel-Yagui, Quality-by-design approach for biological API encapsulation into polymersomes using “off-the-shelf” materials: a study on L-Asparaginase, AAPS PharmSciTech 20 (2019) 1–12.
[37] H. Tseng, J.A. Gage, T. Shen, W.L. Haisler, S.K. Neeley, S. Shiao, J. Chen, P. K. Desai, A. Liao, C. Hebel, et al., A spheroid toxicity assay using magnetic 3D bioprinting and real-time mobile device-based imaging, Sci. Rep. 5 (2015) 1–11.
[38] C.E.M. Krämer, W. Wiechert, Kohlheyer, D. of induced and programmed cell death via non-invasive propidium iodide and counterstain perfusion, Nat. Publ. Gr. (2016) 1–13.
[39] Pustylnikov, S.; Sagar, D.; Jain, P.; Khan, Z.K. Targeting the C-type lectins-mediated host-pathogen interactions with dextran. 2017, 17, 371–392.
[40] Schnatwinkel, C.; Christoforidis, S.; Lindsay, M.R.; Uttenweiler-joseph, S.; Wilm, M. The Rab5 E ector Rabankyrin-5 Regulates and Coordinates Di erent Endocytic Mechanisms. 2004, 1–19.
[41] H.E. Colley, V. Hearnden, M. Avila-Olias, D. Cecchin, I. Canton, J. Madsen, S. MacNeil, N. Warren, K. Hu, J.A. McKeating, et al., Polymersome-mediated delivery of combination anticancer therapy to head and neck cancer cells: 2D and 3D in vitro evaluation, Mol. Pharm. 11 (2014) 1176–1188.
[42] A.T.O. Perform, Lipid peroxidation—DNA damage by malondialdehyde, Fundam. Mol. Mech. Mutagen. 424 (1999) 83–95.
[43] Muramatsu, S.; Suga, Y.; Mizuno, Y.; Hasegawa, T. Differentiation-specific localization of catalase and hydrogen peroxide , and their alterations in rat skin exposed to ultraviolet B rays. 2005, 151–158.
[44] A. Vogt, B. Combadiere, S. Hadam, K.M. Stieler, J. Lademann, H. Schaefer, B. Autran, W. Sterry, Blume-Peytavi, U. 40 nm, but not 750 or 1,500 nm, nanoparticles enter epidermal CD1a+ cells after transcutaneous application on human skin, J. Invest. Dermatol. 126 (2006) 1316–1322.
[45] M.J. Cappel, J. Kreuter, Effect of nonionic surfactants on transdermal drug delivery: II. Poloxamer and poloxamine surfactants, Int. J. Pharm. 69 (1991) 155–167.